Theoretical and Experimental Study of a Quantized Lattice Configuration in a Nearly Unstable Defect System

J. B. Page,[a] J. T. McWhirter, and A. J. Sievers
Laboratory of Atomic and Solid State Physics and Materials Science Center, Cornell University, Ithaca, New York 14853

H. Fleurent, A. Bouwen, and D. Schoemaker
Physics Department, University of Antwerp (UIA), B-2610 Antwerpen (Wilrijk), Belgium
(Received 4 August 1989)

Theoretical lattice-dynamics analysis and new optical experiments on KI:Ag^+ reveal a nearly unstable low-temperature defect-host configuration, whose population decreases dramatically with temperature, but whose dynamics are consistent with a temperature-independent harmonic model involving collective motion. This behavior is in marked contrast to the temperature-dependent evolution of the dynamics of "soft-mode" systems.

PACS numbers: 78.30.−j, 63.20.Pw, 63.20.Ry

The silver ion in KI is the most thermally unstable lattice-defect combination known. At 1.2 K the Ag^+ ion takes the same equilibrium position as the K^+ ion it replaces but by 20 K it is in an off-center position.[1,2] A fundamental problem is to understand within the framework of lattice dynamics how the system moves between these two lattice-defect arrangements with temperature.[3] Missing from the characterization of the dynamics have been complementary temperature-dependent optical and Raman data and a realistic Lifshitz-type calculation of the KI:Ag^+ lattice dynamics.

To experimentally track the temperature dependence of different aspects of the coupled defect-host system, we first present uv measurements which follow the Ag^+ ion itself and then Raman scattering results which monitor the disappearance of the E_g mode and the appearance of a new A_1-symmetry resonant mode as the temperature is raised. Next, the spectral properties of ir- and Raman-active features for the on-center configuration are calculated within the harmonic approximation, and the interplay between theoretical and experimental results is described for the first time. The harmonic approximation is shown to give a good account of the low-temperature ir and Raman data, for a model in which the defect and surrounding host ions remain strongly coupled yet are quite close to being unstable against T_{1u} displacements. Our results imply that the observed temperature dependence of the on-center spectral features simply reflects the population in this state. The system is in either the ground-state configuration or not; a continuous evolution of the on-center defect dynamics with temperature does not occur.

To monitor the position of the Ag^+ ion with temperature we make use of the known optical behavior of this ion in alkali-halide crystals, which can be understood in terms of the $4d^{10} \rightarrow 4d^9 5s$ parity-forbidden transitions of the defect.[4-6] These transitions are made allowed by vibronic couplings to the odd-parity vibrational modes, or if the defect is off center, by the static odd-parity lattice displacement; the larger the odd-parity contribution the larger the line strength.

Figure 1(a) shows the measured uv absorption spectrum of KI:Ag^+ for two different temperatures. Note that over this temperature range the center frequencies remain essentially fixed. A linear concentration depen-

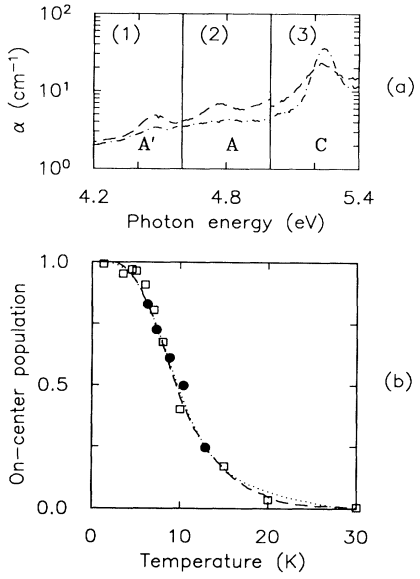

FIG. 1. (a) KI:Ag^+ uv absorption spectra. Dashed line, $T = 50$ K; dot-dashed line, $T = 1.2$ K. Silver concentration: (1) 2×10^{-2} mole%, (2) 2×10^{-3} mole%, (3) 5×10^{-5} mole%. (b) Temperature dependence of Ag^+ on-center population, as determined by various measuring techniques. Dashed line, fir resonant- and gap-mode data, Ref. 1. Dotted line, dielectric constant data, Ref. 2. Squares, uv absorption, A' mode, see text. Circles, Raman scattering, see text.

dence establishes that these three features, labeled A, A', and C in the nomenclature of Ref. 4, are associated with isolated Ag^+ ions.[7] To display the three lines in one figure, three different Ag^+ concentrations are required as described in the caption. The strength of the strong uv line C shown in Fig. 1(a) is temperature independent, and it is assigned to a delocalized excitation involving electron transfer from a nearest-neighbor anion. The weak lines A and A' are assigned to the $A_{1g}(4d^{10}) \rightarrow T_{2g}(4d^9 5s)$ and $A_{1g}(4d^{10}) \rightarrow E_g(4d^9 5s)$ transitions, respectively. They display very little strength at 1.2 K but grow rapidly with increasing temperature. The change is much faster than can be obtained from the occupation-number effect in the T_{1u} resonant mode.

We find that the increase in optical strength of A and A' with temperature is identical to that found earlier for the increase in the dc dielectric constant produced by the appearance of the permanent dipole moment with increasing temperature. This latter change was shown[2] to be proportional to the population P_{off} in the off-center configuration. By letting $P_{\text{on}} = 1 - P_{\text{off}}$, both the uv (squares) and dielectric-constant (dotted line) data can be compared directly with the value of P_{on} determined from the temperature dependence of the strengths of the T_{1u} resonant and gap modes (dashed line).[1] These results are graphed in Fig. 1(b). All three experimental probes consistently measure the same rapid change in the population of the on-center configuration.

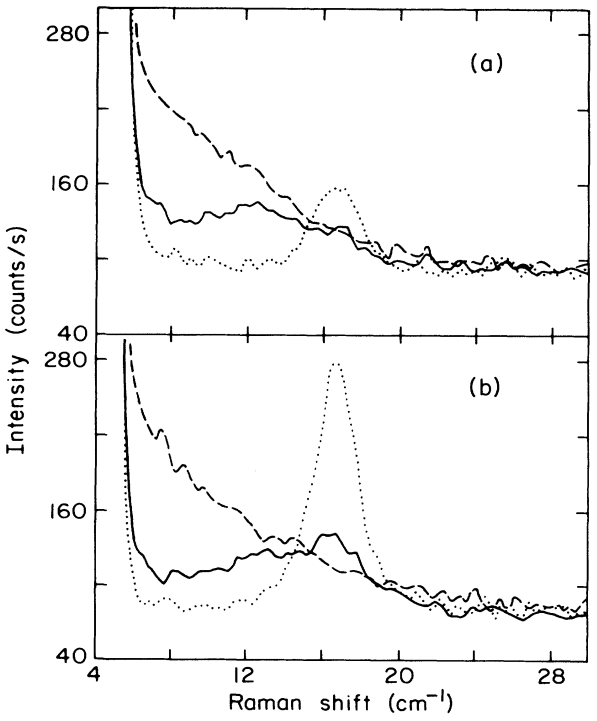

FIG. 2. Temperature dependence of the polarized Raman spectra of a {110}-polished KI+0.3% AgI crystal. The spectra, taken with 488-nm excitation (200 mW), are displayed for two polarization geometries: (a) $\langle 1,-1,0\rangle\langle 1,-1,0\rangle$ and (b) $\langle 1,1,0\rangle\langle 1,-1,0\rangle$. The three temperatures shown are 6.3 (dotted line), 12.9 (solid line), and 25.2 K (dashed line). No $\langle 1,-1,0\rangle\langle 0,0,1\rangle$ polarized lines were observed at any temperature. The statistical fluctuations are about 15 counts/s. The resolution is 2.5 cm^{-1}.

The polarized Raman intensities $I(\langle 1,-1,0\rangle\langle 1,-1,0\rangle)$, $I(\langle 1,1,0\rangle\langle 1,-1,0\rangle)$, and $I(\langle 1,-1,0\rangle\langle 0,0,1\rangle)$ were recorded in the 90° scattering geometry. The results for the first two polarizations are shown in Figs. 2(a) and 2(b). No impurity-induced scattering was observed for the third orientation. The data are classified according to the representations A_{1g}, E_g, and T_{2g} of the cubic group O_h, which yields for the polarized intensities the expressions

$$I(\langle 1,-1,0\rangle\langle 1,-1,0\rangle) = A_{1g} + \tfrac{1}{4}E_g + \tfrac{1}{2}T_{2g},$$

$$I(\langle 1,1,0\rangle\langle 1,-1,0\rangle) = \tfrac{3}{4}E_g,$$

$$I(\langle 1,-1,0\rangle\langle 0,0,1\rangle) = \tfrac{1}{2}T_{2g}.$$

The Raman measurements presented in Fig. 2 support the low-temperature E_g-mode frequency assignment of Kirby.[8] On the other hand, neither of his previously proposed A_{1g} and T_{2g} resonances are observed. A new discovery is the strong temperature dependence of the Raman scattering. As temperature is increased, the scattering strength of the 16.1-cm^{-1} E_g mode decreases rapidly [see the circles in Fig. 1(b)], yet its center frequency stays nearly fixed. The temperature dependence of this Raman line is similar to that of the ir (Ref. 1) and the optical features discussed above, but it takes on added importance because the E_g mode involves no motion of the Ag^+ ion. In addition, a new mode showing both E_g and A_{1g} components grows in strength at 12.0 cm^{-1}. A "behavior-type" analysis[9] of its polarized Raman intensities is consistent with a C_{4v}:A_1 symmetry mode. At still higher temperatures this feature disappears (or broadens) into an increasing central feature having the same polarization properties, and likely produced by the off-center tunneling levels themselves. The mode frequencies are given in Table I.

TABLE I. Measured and calculated frequencies (in cm^{-1}) for the ir- and Raman-active modes of KI:Ag^+ for two different configurations. The frequencies used to fix the two force-constant parameters of the model are underlined.

Mode symmetry	On-center Expt.	On-center Theory	Off-center Expt.
T_{1u}	17.3	<u>17.3</u>	Tunneling
T_{1u}	86.3	<u>86.3</u>	78.6
E_g	16.1	20.6	12.0
A_{1g}	Unobserved (see text)	37.4	12.0

The low-temperature perturbed lattice dynamics are computed in the harmonic approximation using the Lifshitz method[10] and employing realistic breathing-shell-model[11] host-crystal phonons to calculate the required Green's-function elements. In this approach, both low-frequency in-band resonances and localized modes are given by the solution of

$$\mathrm{Re}\,|\mathbf{I}+\mathbf{g}_0(z)\mathbf{c}(z)|=0\,, \tag{1}$$

where $\mathbf{c}(z)\equiv\Delta\Phi-z\Delta\mathbf{m}$ is the defect-space perturbing matrix, defined in terms of the changed force-constant and mass matrices; $z\equiv\omega^2+i0^+$, where ω is the frequency; and $\mathbf{g}_0(z)\equiv(\Phi_0-z\mathbf{m}_0)^{-1}$ is the defect-space harmonic Green's-function matrix.

Our model for the perturbing matrix incorporates, in addition to the known $\Delta\mathbf{m}$, defect–first-neighbor and relaxation-induced first-neighbor–fourth-neighbor longitudinal force-constant changes δ and δ', illustrated in the inset of Fig. 3. For the linear concentration regime we treat the case of a single defect. For this assumed low-temperature on-center configuration, the site symmetry is O_h, and our model results in the perturbed phonons being of just the symmetry types T_{1u} (infrared active) or A_{1g} and E_g (both Raman active).

Our Raman calculations are based on the usual theory for defect-induced off-resonance Raman scattering.[12] In the absence of defects, first-order scattering from the host crystal is forbidden since every site has inversion symmetry. With a defect present we compute the first-order A_{1g} and E_g spectra assuming that the only nonzero electronic polarizability derivatives involve longitudinal motion of the defect's six-nearest neighbors. This results in two independent polarizability derivatives. Their values depend on the details of the coupling of the impurity's electronic states to the perturbed phonons, and they have not been computed.

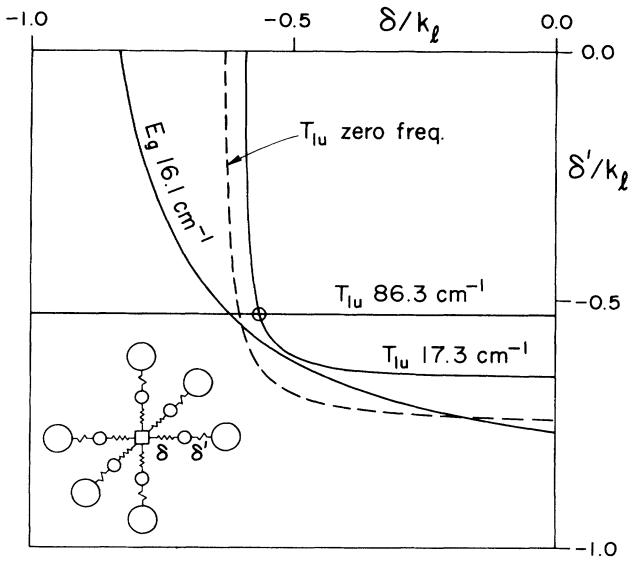

FIG. 3. Calculated fractional force-constant changes for resonances and gap modes at fixed frequencies. Inset: The force-constant perturbations in our model; all other short-range and Coulomb force constants are unperturbed. The fractional changes are given in units of the pure KI breathing-shell-model nearest-neighbor longitudinal overlap force constant $k_1=1.884\times10^4$ dyn/cm. The dashed curve is for a T_{1u} instability.

To calculate the infrared absorption one must take account of the fact that the radiation can couple to all of the ions in the system. For the case when the impurity may be regarded as having the same effective charge as the replaced ion, and assuming the standard Lorentz local field correction to hold, Klein[13] has shown that the impurity-induced absorption is proportional to the imaginary part of the defect space $\mathbf{t}$ matrix defined by $\mathbf{t}(z)\equiv\mathbf{c}(z)[\mathbf{1}+\mathbf{g}_0(z)\mathbf{c}(z)]^{-1}$.

Our procedures for computing the required unperturbed Green's-function elements from the host-crystal phonons are the same as detailed in Refs. 12 and 14, except that we used the equivalent of one million wave vectors in the Brillouin zone (22932 wave vectors in the irreducible $\frac{1}{48}$ volume element of the Brillouin zone), and the imaginary parts of the unperturbed Green's functions were computed as histograms using 100 bins of equal width in frequency. The two model parameters δ and δ' were chosen to reproduce the observed (ir) frequencies of the T_{1u} modes listed in Table I. The resulting fractional force-constant changes are $\delta/k_1=-0.564$ and $\delta'/k_1=-0.528$. Our model then predicts an E_g resonance at 20.6 cm^{-1} and an A_{1g} resonance at 37.4 cm^{-1}, as well as a gap mode of each of these symmetries. The predicted E_g resonance is in reasonable agreement with the 16.1-cm^{-1} E_g resonance observed in Raman scattering. Although the predicted A_{1g} resonance is not observed in the measured Raman spectra, the A_{1g} and E_g Raman strengths are independently determined by the two undetermined electronic polarizability derivatives. Thus the null A_{1g} experimental result could be used to place bounds on these derivatives.

Additional tests of the model can be made by computing the relative strengths of the predicted gap modes and resonances, within a given spectrum. The result for the calculated T_{1u} modes is $S(86.3)/S(17.3)=1.4$, in reasonable agreement with the experimental value of ~3. The predicted A_{1g} and E_g gap-mode strengths in the Raman spectra are, relative to the predicted strengths of the low-frequency A_{1g} and E_g resonances, too weak to be observed, and no Raman-active gap modes have been seen.

In order to give a better overall perspective of our theoretical results, we plot in Fig. 3 curves of δ/k_1 vs δ'/k_1 obtained by solving Eq. (1) for resonant or gap modes at four frequencies. Each of these quantities is allowed to vary over the range $(-1,0)$, appropriate to substantial force-constant softening. All the values $(\delta/k_1,\delta'/k_1)$ on a given curve produce a mode of the in-

dicated type and frequency. The intersection of the curves for the 17.3-cm^{-1} T_{1u} resonance and the 86.3-cm^{-1} T_{1u} gap mode, shown by the circle in Fig. 3, gives our parameter values used above. The dashed curve is for the case of a T_{1u} resonance at *zero* frequency, so that the values of $(\delta/k_1,\delta'/k_1)$ on this curve correspond to the on-center configuration being unstable against T_{1u} displacements—as detailed in Ref. 14, the long-range Coulomb force constants, unperturbed in our model, result in significant displacements of the host-lattice ions in the mode patterns for these instabilities. We have found that the T_{1u} resonance is almost always the first to become unstable as the force constants are softened; as a result, only the portion of the figure to the upper right of the dashed curve is physically reasonable, although Eq. (1) has solutions outside this range.

The picture resulting from our experiments and theoretical analysis is that of a nearly unstable low-temperature defect-host configuration whose dynamics are explained within the harmonic approximation but whose population decreases dramatically with temperature. Thermal energy does not appear to modify the ground-state dynamics. This behavior is in sharp contrast with that of "soft-mode" systems, which also involve nearly unstable collective motion, but with dynamics that evolve continuously with temperature. Thus an approach fundamentally different from those for soft-mode systems is required (see, for example, Ref. 15 for one such possibility).

Work by J.B.P., J.T.M., and A.J.S. was supported by ARO-DAAL03-86-K-0103 and by NSF-DMR-88-18558 while that by H.F. was supported by Nationaal Fonds voor Wetenschappelijk Onderzoek (Belgium) and that by A.B. and D.S. by Interuniversitair Instituut voor Kernwetenschappen (Belgium).

[a]Permanent address: Department of Physics, Arizona State University, Tempe, AZ 85287.

[1]A. J. Sievers and L. H. Greene, Phys. Rev. Lett. **52**, 1234 (1984).

[2]S. B. Hearon and A. J. Sievers, Phys. Rev. B **30**, 4853 (1984).

[3]A related two-configuration system has been obtained by applying hydrostatic pressure to RbCl:Ag$^+$; see, F. Bridges, M. Reece, and M. Morgan, Radiat. Eff. **73**, 31 (1983); F. Bridges and D. Chow, Phys. Rev. Lett. **54**, 1532 (1985).

[4]K. Fussgänger, Phys. Status Solidi (b) **34**, 157 (1969); **36**, 645 (1969).

[5]K. Kojima, M. Sakurai, and T. Kojima, J. Phys. Soc. Jpn. **24**, 815 (1968).

[6]U. Holland and F. Luty, Phys. Rev. B **19**, 4298 (1979).

[7]Because the AgI precipitation effect was not understood in the early work, our results differ appreciably from those reported in Refs. 4 and 5.

[8]R. D. Kirby, Phys. Rev. B **4**, 3557 (1971).

[9]J. F. Zhou, E. Goovaerts, and D. Schoemaker, Phys. Rev. B **29**, 5509 (1984).

[10]General aspects of the theory of perturbed phonons are reviewed in H. Bilz, D. Strauch, and R. K. Wehner, *Handbuch der Physik* (Springer-Verlag, Berlin, 1984), Vol. XXV, Pt. 2d.

[11]U. Schröder, Solid State Commun. **4**, 347 (1966).

[12]See, for instance, R. T. Harley, J. B. Page, and C. T. Walker, Phys. Rev. B **3**, 1365 (1971), and references therein.

[13]M. V. Klein, in *Physics of Color Centers,* edited by W. B. Fowler (Academic, New York, 1968), p. 464.

[14]J. B. Page, Phys. Rev. B **10**, 719 (1974); J. B. Page and K. G. Helliwell, Phys. Rev. B **12**, 718 (1975).

[15]A. J. Sievers and S. Takeno, Phys. Rev. Lett. **61**, 970 (1988).